



Liquid Crystal Infiltration of Template Patterned 3D Photonic Crystals

**E. Graugnard, D. P. Gaillot, J. S. King, S. Jain
& C. J. Summers**

*School of Materials Science and Engineering
Georgia Institute of Technology, Atlanta, GA*

Y. Zhang-Williams & I. C. Khoo

*Department of Electrical Engineering
Pennsylvania State University, University Park, PA*

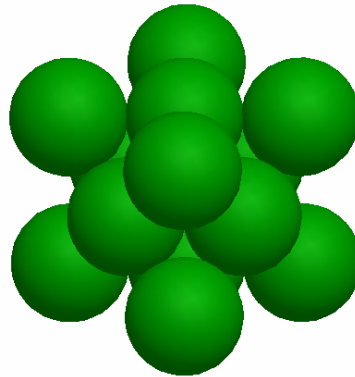
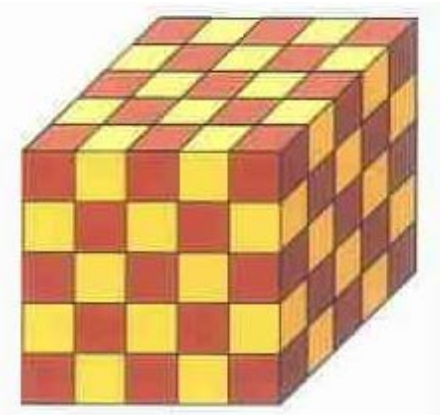


-
- 3D Photonic Crystals
 - Review of Liquid Crystals in 3D Photonic Crystals
 - Tunability Schemes
 - **Tunability Computations (FDTD)**
 - Opal
 - Inverse shell opal
 - Non-close-packed inverse opals
 - **Experimental Studies**
 - Non-close-packed inverse opals
 - Pre-Sinter plus Atomic layer deposition (ALD)
 - Liquid crystal infiltration – 5CB
 - Reflectance Spectra
 - Electric field tuning
 - Hydrophobic / Hydrophilic
 - Summary

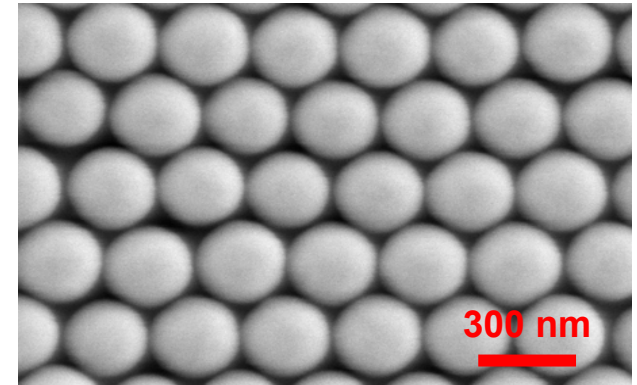
3D Photonic Crystals



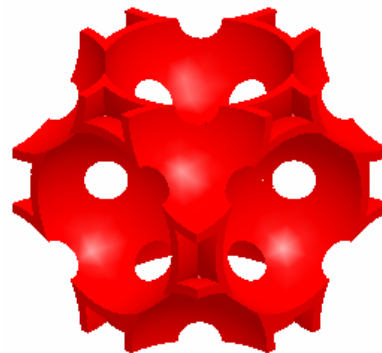
Opals



26% air

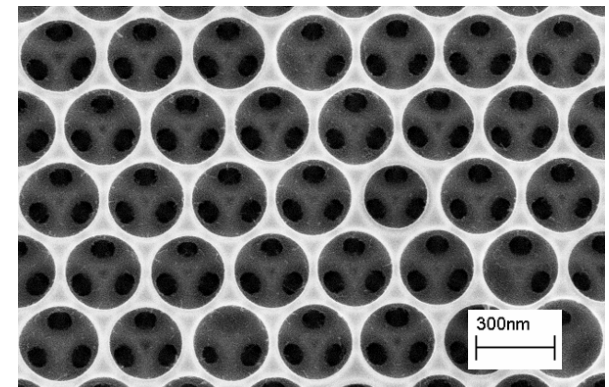


Structures with a
3-dimensional
dielectric
periodicity.



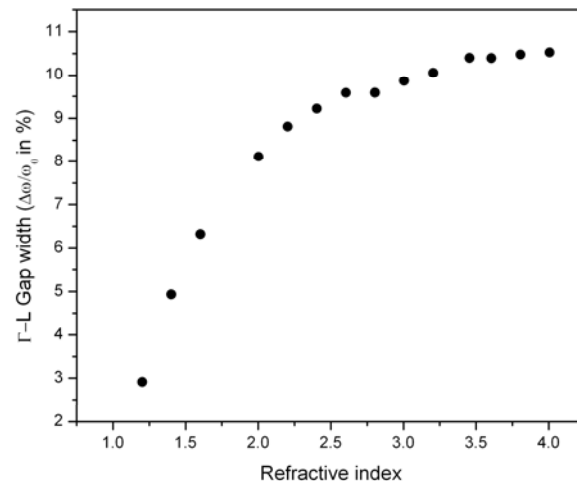
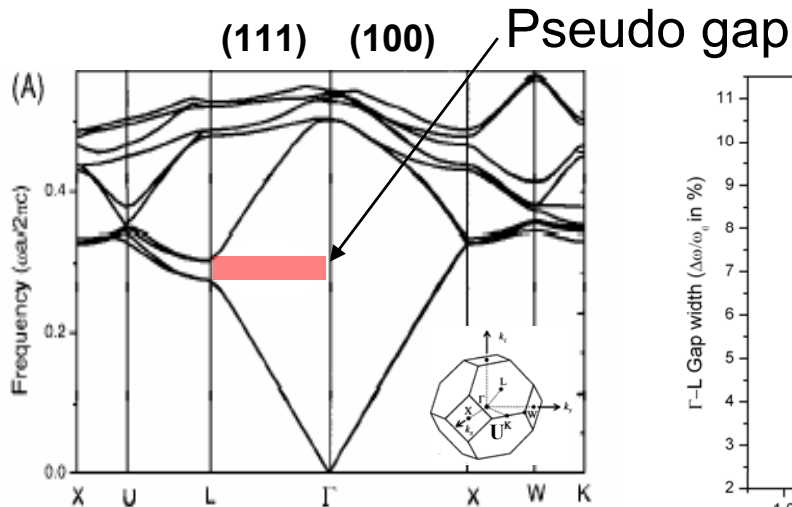
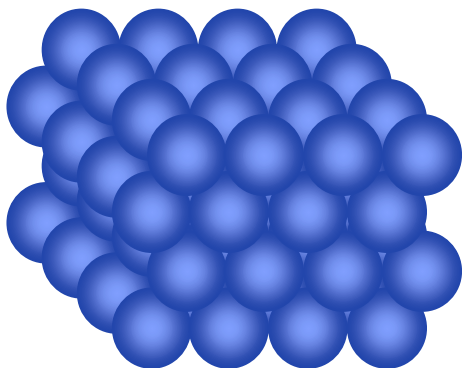
77.4% air

Inverse opals

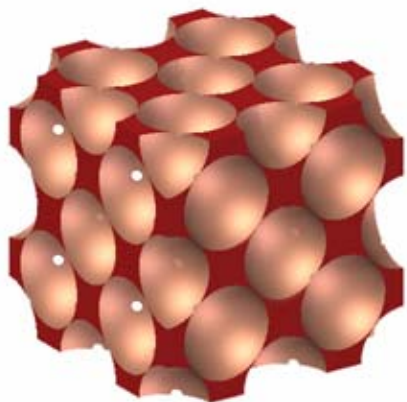




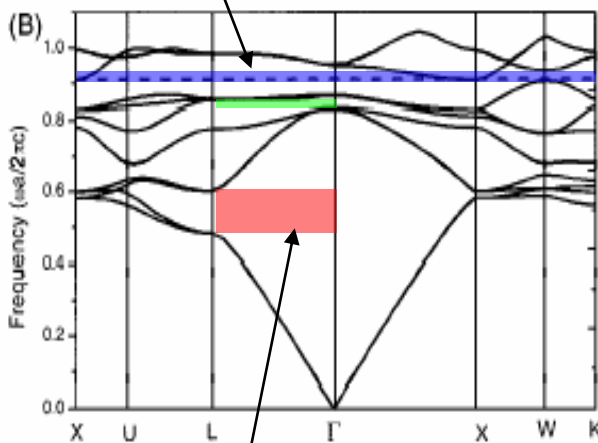
Opals:



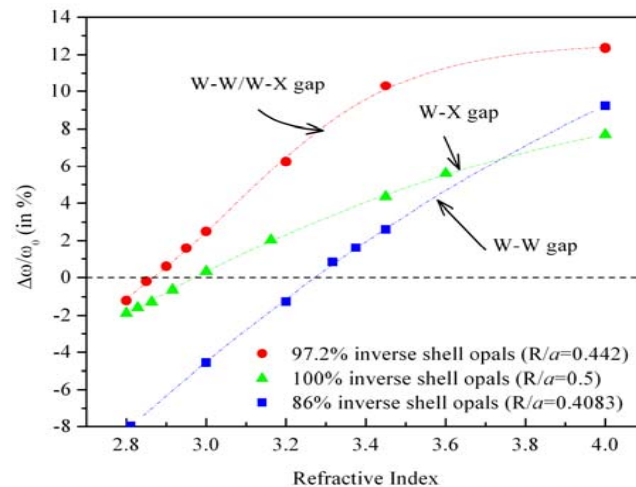
Inverse opals:



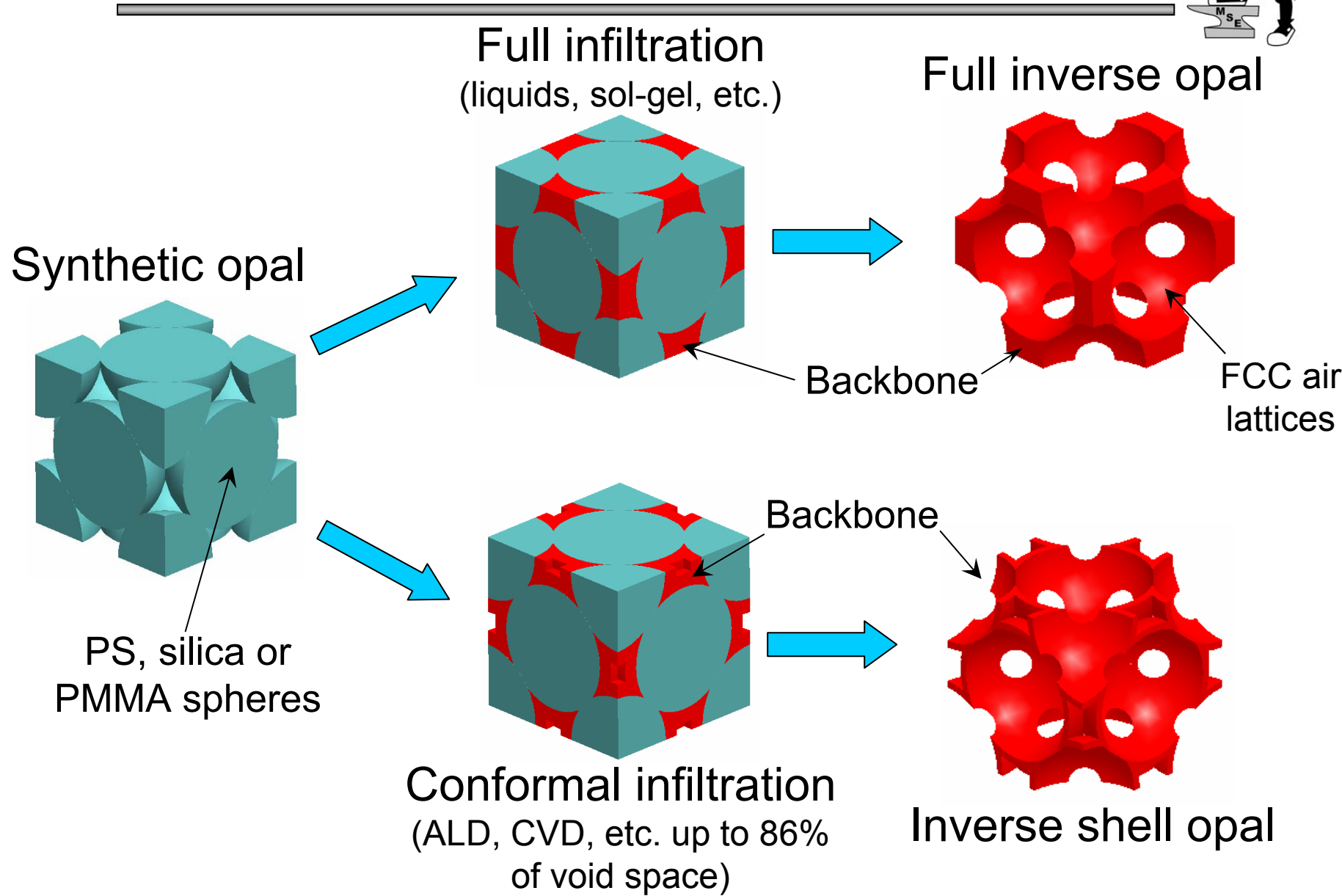
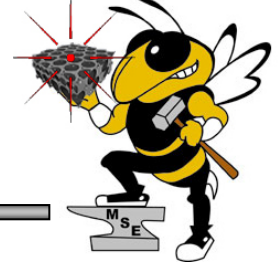
Full gap possible



Pseudo gap



Inverse Opal Structures



Properties of Opals and Inverse Opals



- **Opals**
 - 2-3 Γ -L Pseudo PBGs observed for refractive index greater than 1.1 (PS, silica, PMMA colloidal spheres)
- **Conformally infiltrated opals (ALD/CVD techniques)**
 - Total dielectric volume $< 26\%$ ($\sim 22.4\%$)
 - Outer shell radius controls final geometry
 - PBG static tunability is a function of lattice constant a , refractive index contrast and dielectric filling fraction
- **Inverse shell opals**
 - Complete PBG predicted for $n > 3.3$ (Si, GaP, etc.)
 - FCC air lattices reported to enhance PBG properties
 - Total dielectric volume $< 26\%$ ($\sim 22.4\%$)
 - PBG static tunability is a function of lattice constant a , backbone refractive index, dielectric filling fraction and network topology

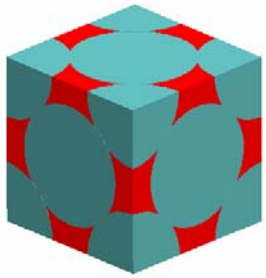


-
- **Liquid crystal tuning in infiltrated opals:**
 - K. Yoshino *et al.* Appl. Phys. Lett. 75, 932 (1999)
 - K. Yoshino *et al.* Synth. Metals 121, 1459 (2001)
 - D. Kang *et al.* Phys. Rev. Lett. 86, 4052 (2001)
 - Q.-B. Meng *et al.* J. Appl. Phys. 89, 5794 (2001)
 - Y. Shimdo *et al.* Appl. Phys. Lett. 79, 3627 (2001)
 - **Liquid crystal infiltration in inverse opals:**
 - K. Busch & S. John, PRL 83, 967 (1999)
 - P. Mach *et al.* Phys. Rev. E 65, 031720 (2002)
 - G. Mertens *et al.* Appl. Phys. Lett. 80, 1885 (2002)
 - M. Ozaki *et al.* Adv. Mater. 14, 514 (2002)
 - S. Kubo *et al.* J. Am. Chem. Soc. 124, 10950 (2002)
 - S. Gottardo *et al.* Physica B 338, 143 (2003)
 - S. Kubo *et al.* J. Am. Chem. Soc. 126, 8314 (2004)
 - S. Kubo *et al.* Chem. Mater. 17, 2298 (2005)

Tunability Schemes

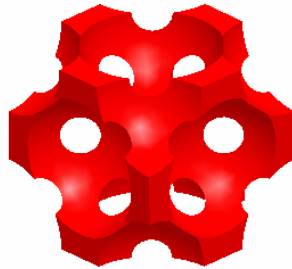


LC Infiltrated Opal

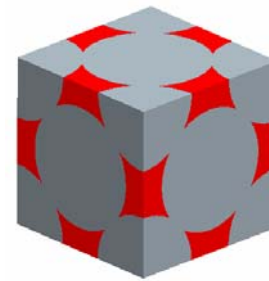


Tunable fully infiltrated opal (backbone material)

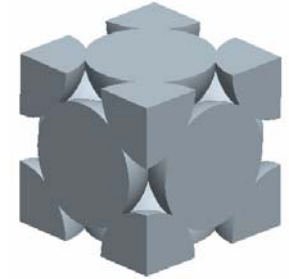
PLZT Inverse Opal



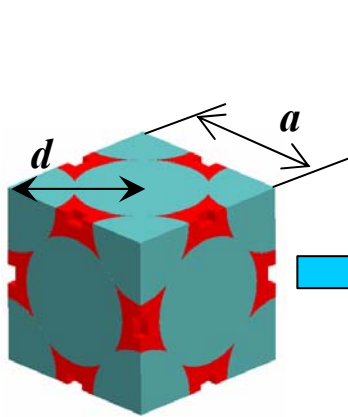
Tunable inverse opal



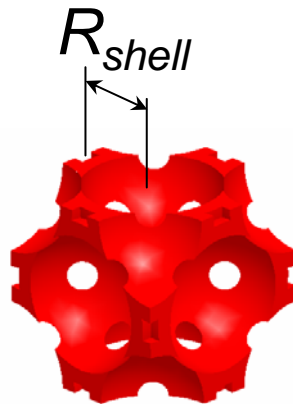
Tunable fully infiltrated inverse opal



Tunable opal

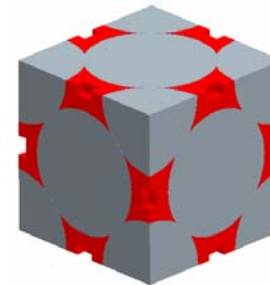


Tunable partially infiltrated opal (backbone material)



Tunable inverse shell opal

LC Infiltrated Inverse Opal



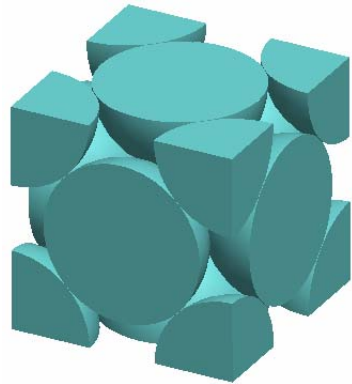
Partially infiltrated ($R_{shell}/a > 0.4083$)

Tunable liquid/solid material

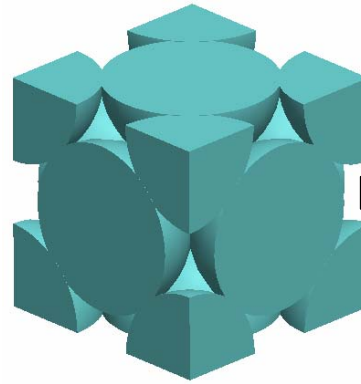
Non-close-packed Inverse Shell Opals



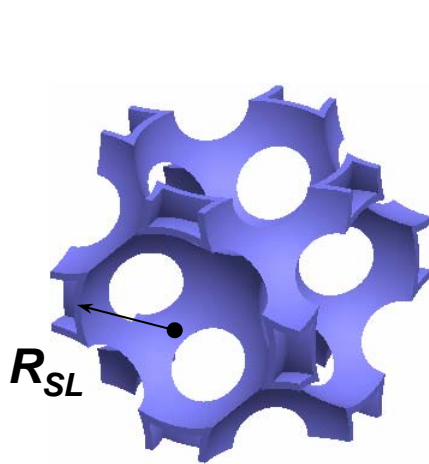
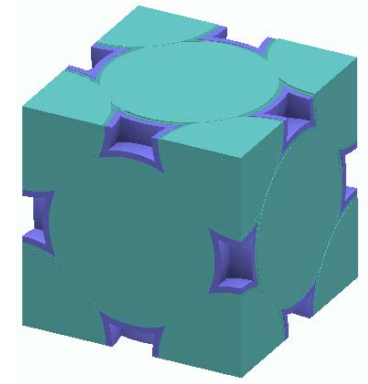
Opal Template



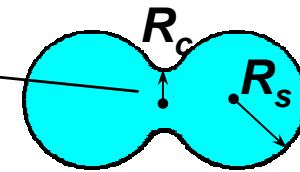
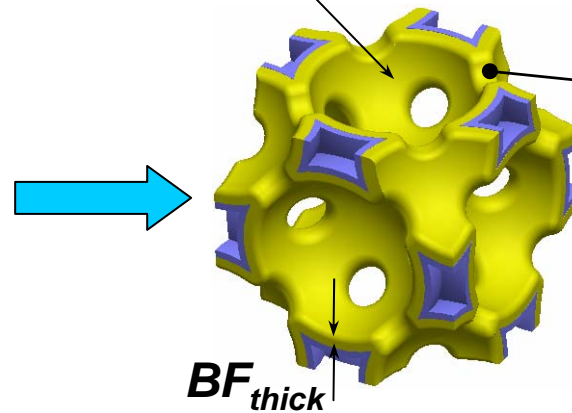
Sintered



Infiltrated



Backfill layer



$$R_s = R_{SL} - BF_{thick}$$

$$R_c^2 = \sqrt{(R_{SL}^2 - R^2) - BF_{thick}}$$

M. Doosje *et al.* J. Opt. Soc. Am. B 17, 600 (2000)

H. Miguez *et al.* Adv. Mater. 15, 597 (2003)

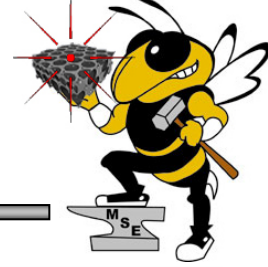
Properties of Non-close-packed Inverse Shell Opals



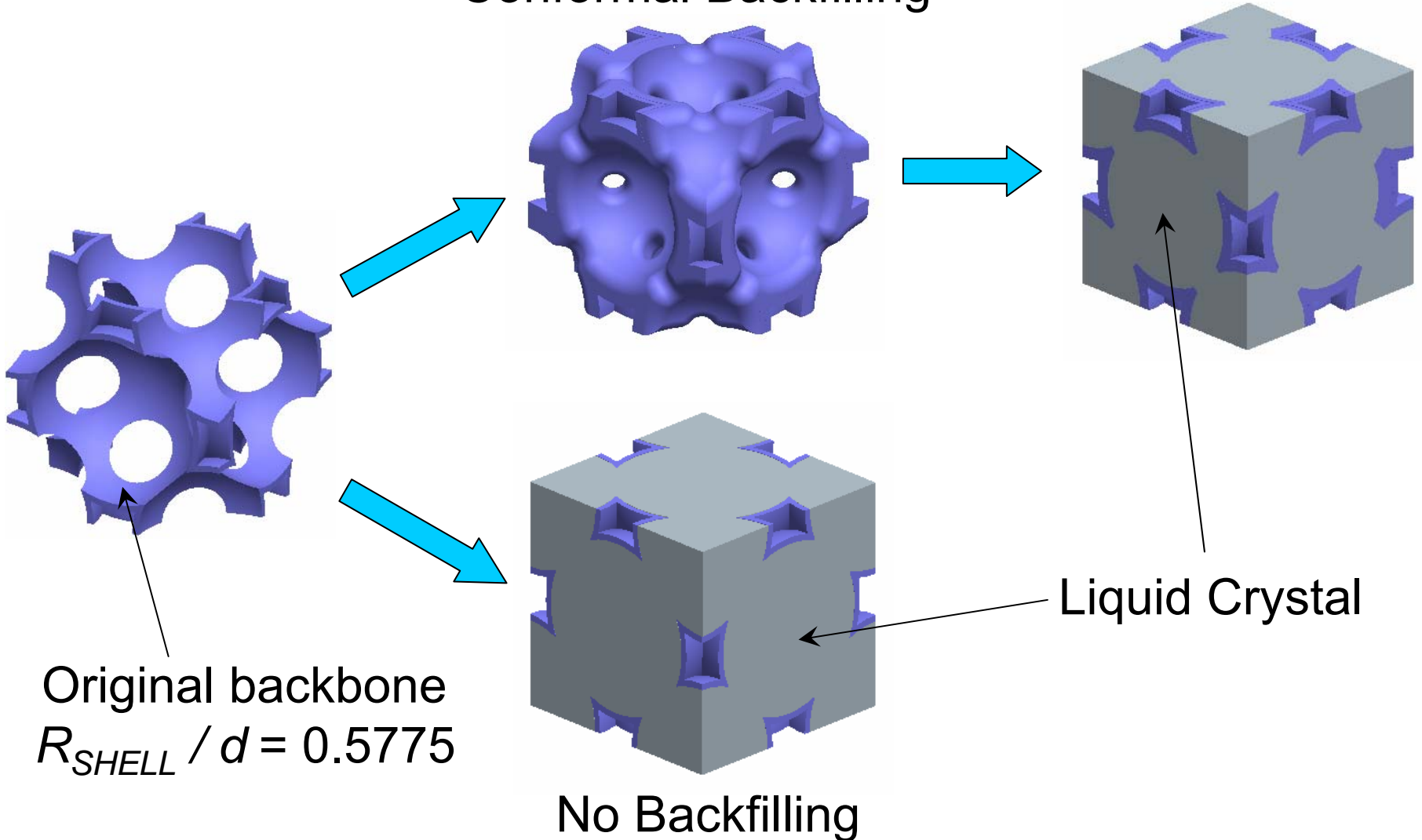
- **Non-close-packed inverse shell opals***
 - Complete PBG predicted for $n > 2.6$ in optimized structures
 - Lowest possible dielectric filling fraction (~5%)
 - Highest open volume available for infiltrated material (up to ~95%)
 - Outer shell radius and backfill thickness control final geometry and degree of connectivity
 - Wide air pores offer electro-optical material infiltration ease
 - ALD technique supports fine network topology tuning thus enabling tailoring of PBG properties
 - Structures resulting to sintered opals-like are achievable using various materials

*Gaillet *et al.* (to be submitted)

Non-close-packed Inverse Shell Opal Tunability Schemes



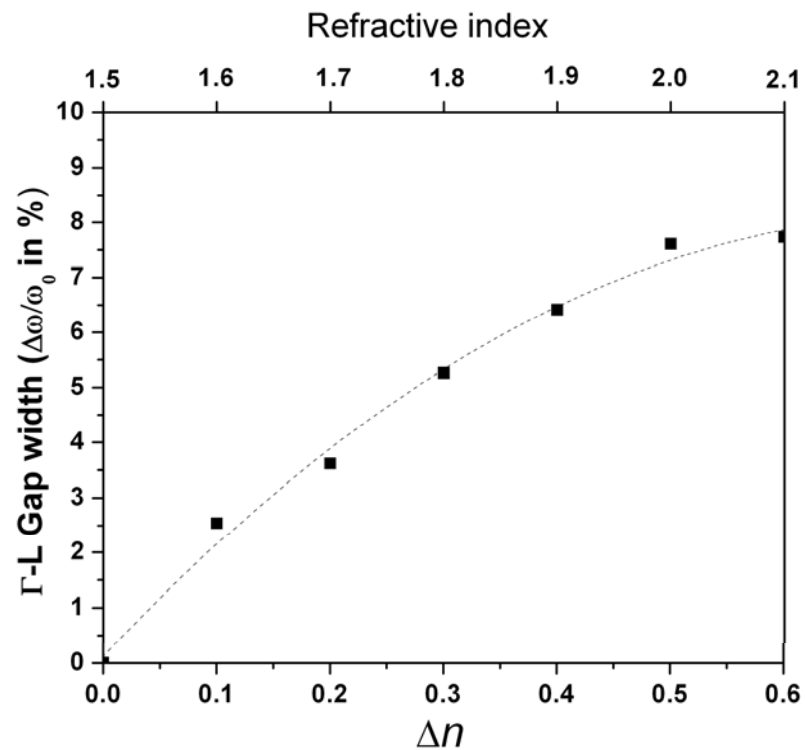
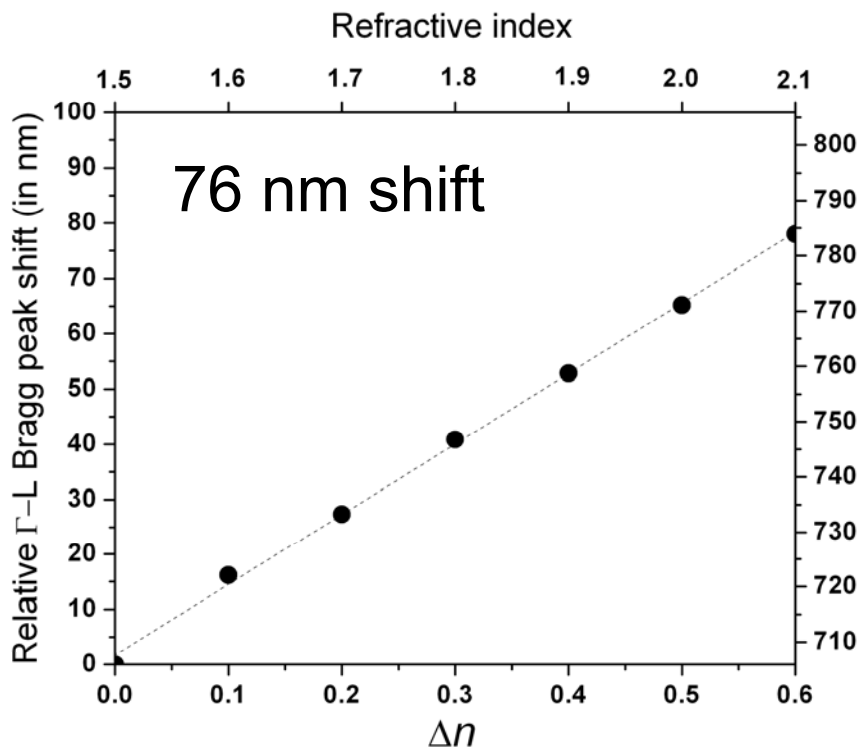
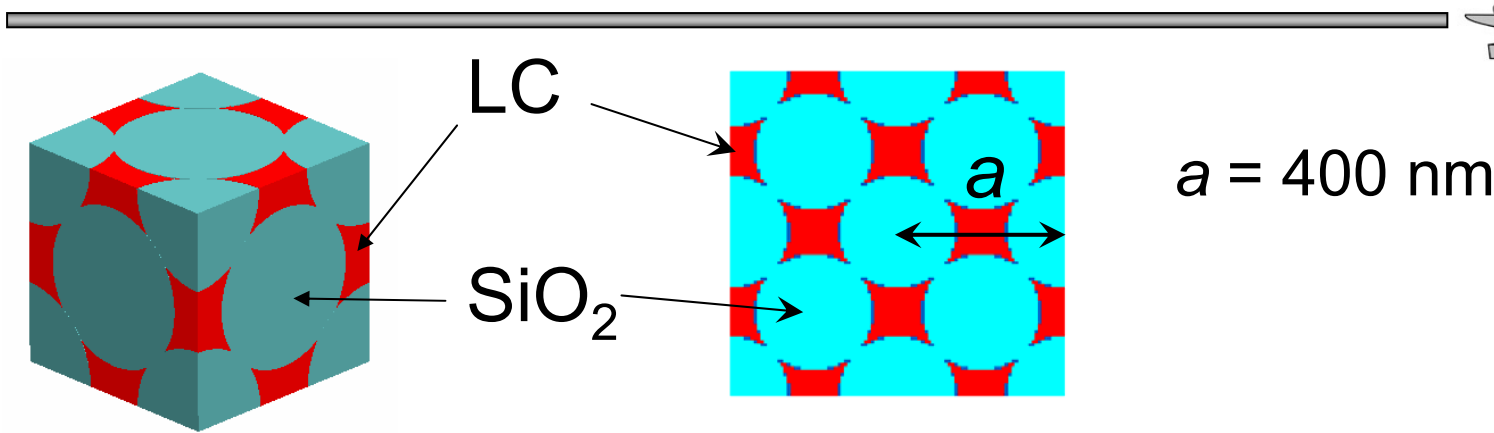
Conformal Backfilling



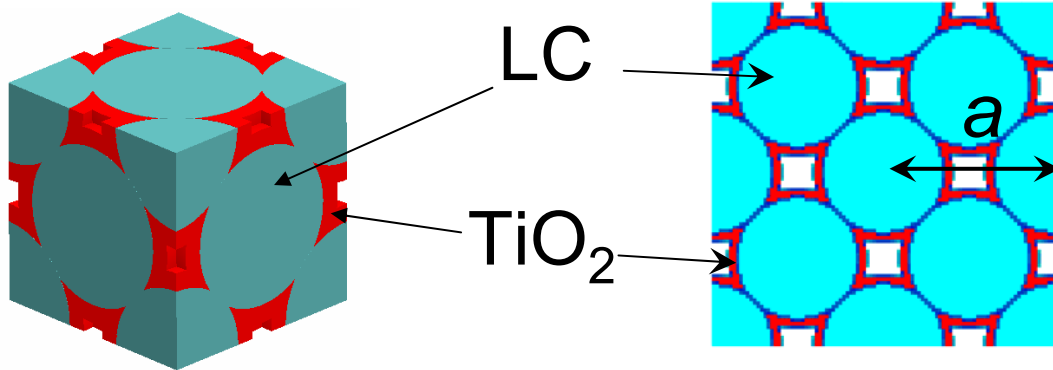


-
- 3D-finite difference time domain (3D-FDTD) was used as a robust and versatile technique to compute photonic properties.
 - Photonic bands for the Γ -L k -vector domain were computed to predict gap widths and central positions of 1st order Bragg peak.
 - Structures investigated:
 - Opals
 - Inverse opals/shell opals
 - Non-close-packed inverse opals and related
 - Tunable materials investigated:
 - Liquid Crystal (LC) with $n = 1.5$ - 2.1 ($\Delta n = 0.6$)

LC Infiltrated Silica Opals

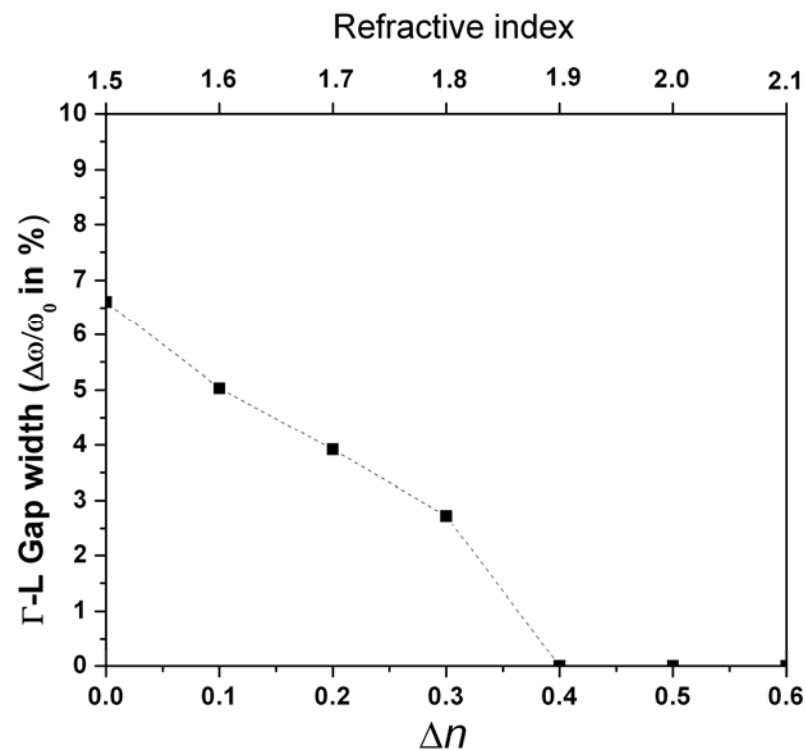
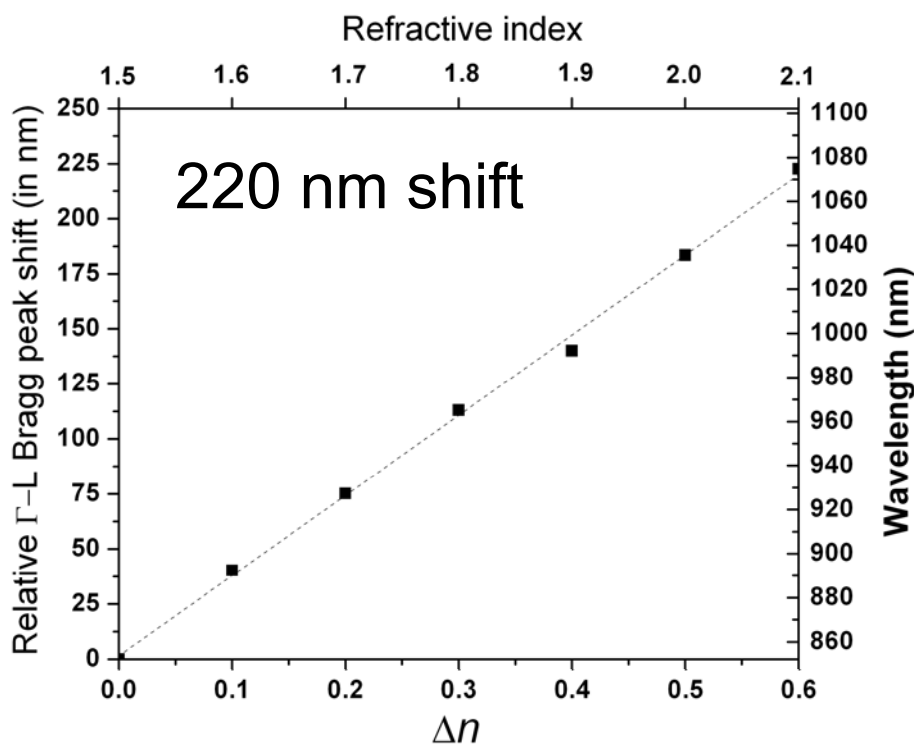


LC Infiltrated TiO₂ Inverse Shell Opals

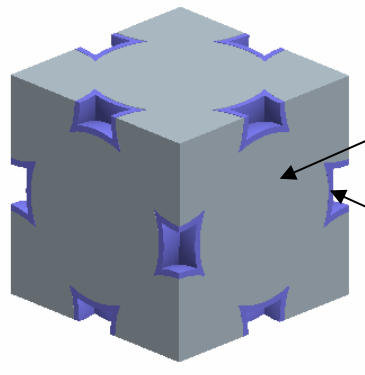
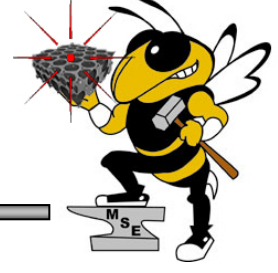


$$a = 400 \text{ nm}$$

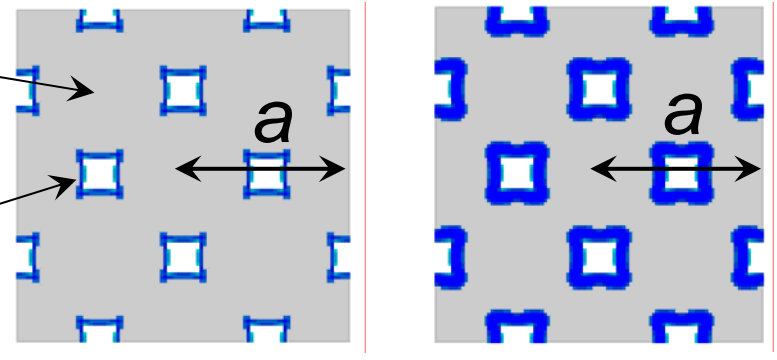
$$n_{\text{TiO}_2} = 2.65$$



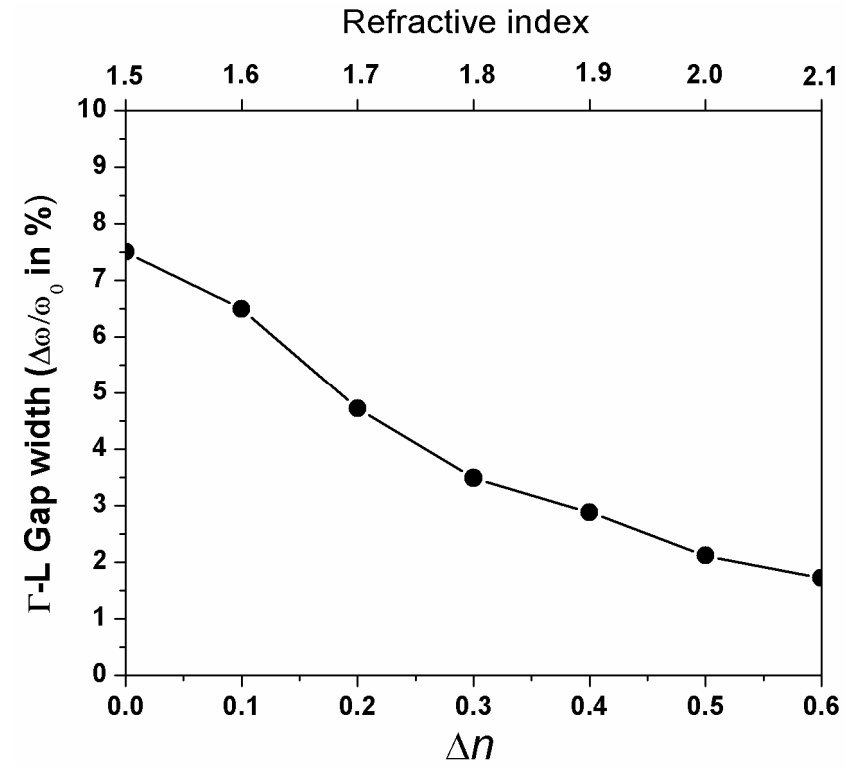
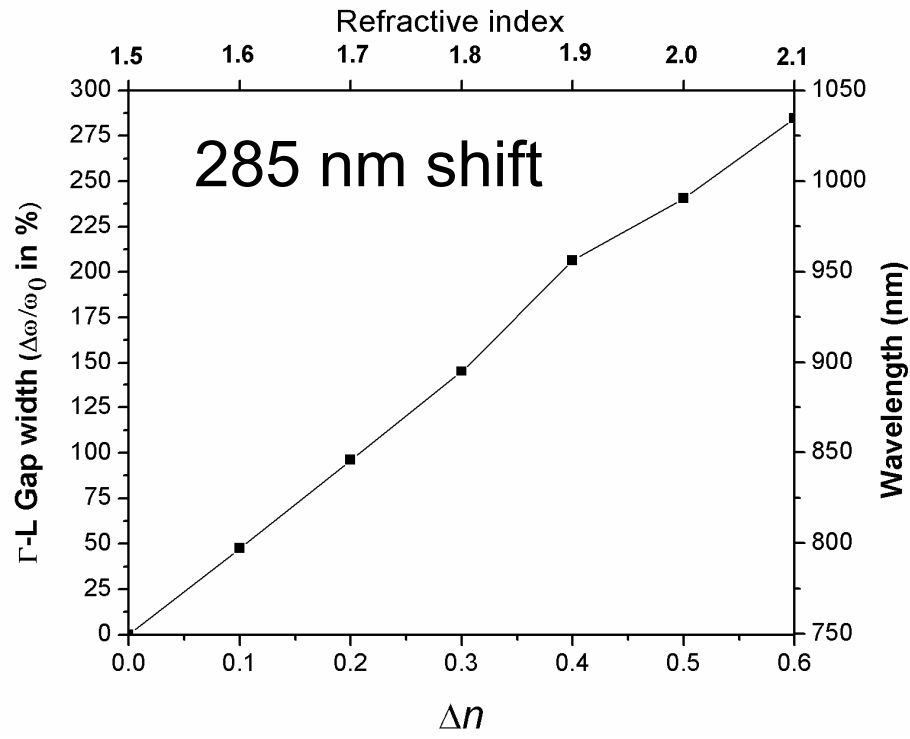
LC Infiltrated Non-close-packed Inverse Shell Opals



LC
TiO₂

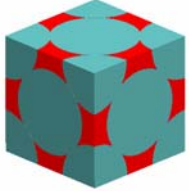

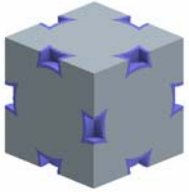



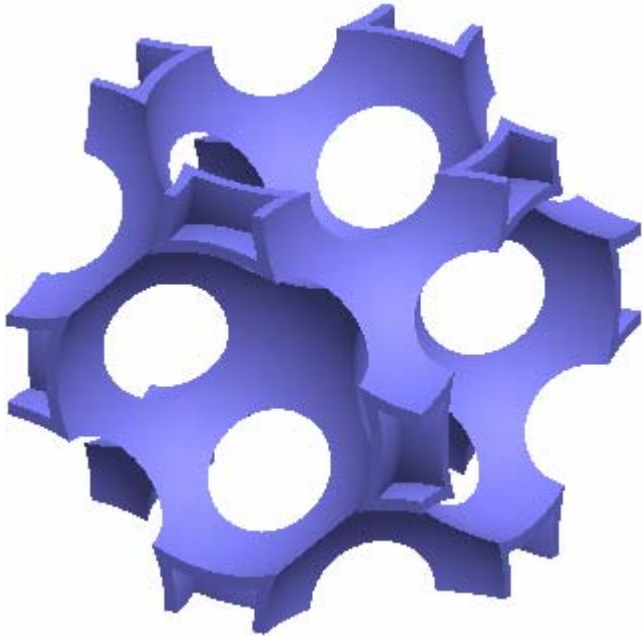
$a = 400 \text{ nm}$



LC Tunability Results

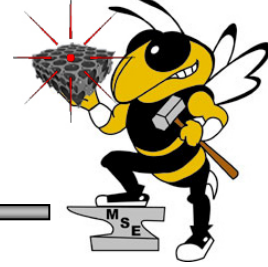


	Structure	Max. PBG width (%)	PBG width tunability – $\Delta n = 0.1$ (%)	Γ -L Bragg peak shift – $\Delta n = 0.1$ (nm)	Maximum Volume (%)
SiO ₂ Opals		8	1.5	13	26
TiO ₂ Inverse shell opals		6.6	1.5	37	74
Non-close-packed inverse shell opals		2.1	1	47	90.5
Non-close-packed inverse shell backfilled opals		7.5	1.5	35	68.6

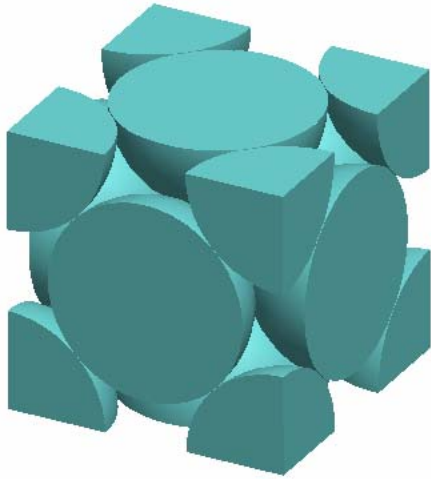


- Non-close-packed inverse shell opal structures
- Lowest dielectric filling fraction
- Large volume available for liquid crystal
- Largest shift of the Bragg peak

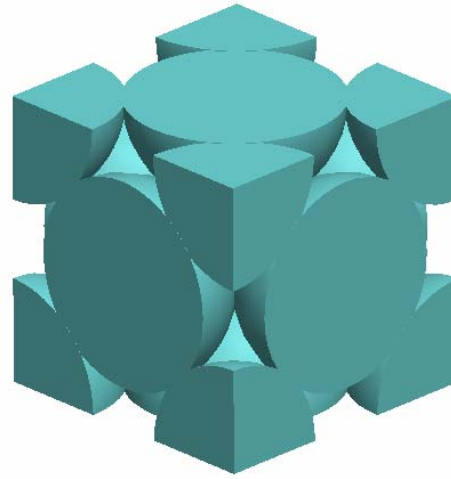
Fabrication of Non-close-packed Inverse Shell Opals



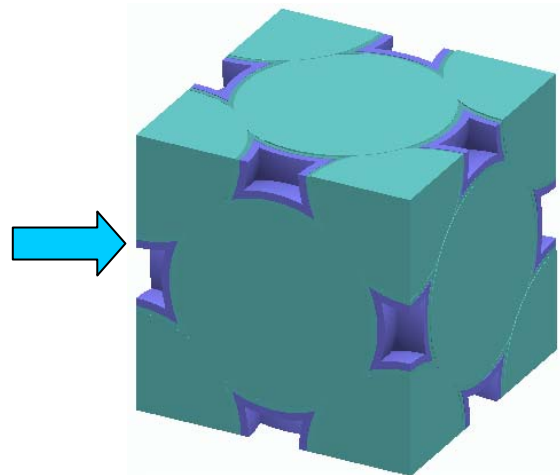
Opal Template



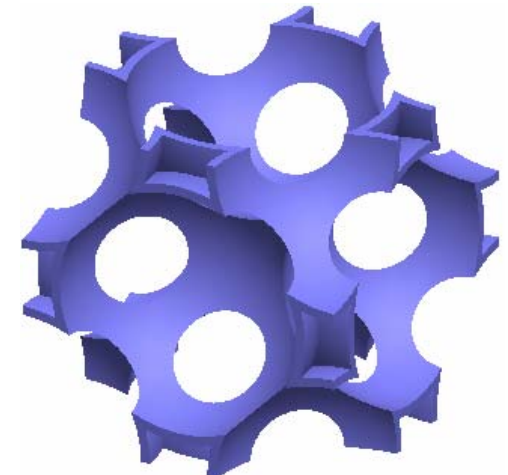
Sintered



Infiltrated



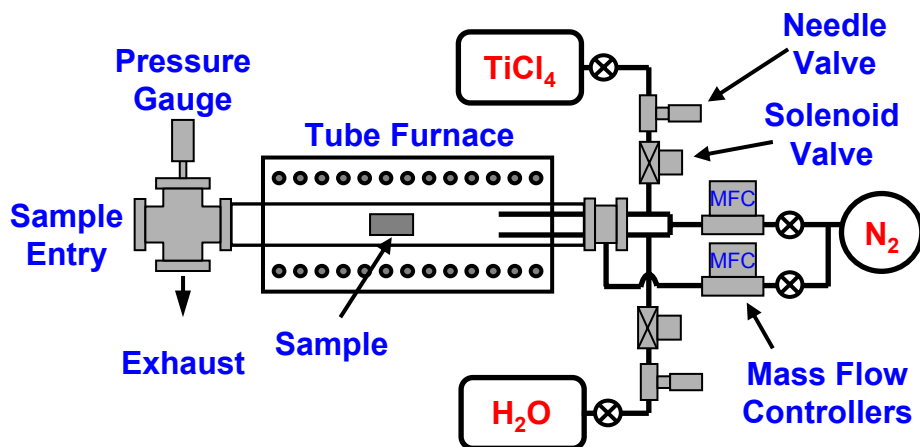
Inverted



NCP Inverse Opal Fabrication: Atomic Layer Deposition



- Atomic layer deposition in synthetic opal templates using TiO_2 and Al_2O_3 .
- Surface limited growth.
- Precise digital control of film thickness.
- Low temperature growth (80°C) allows
 - Ultra-smooth conformal thin films
 - growth on PS spheres
- Selective etching

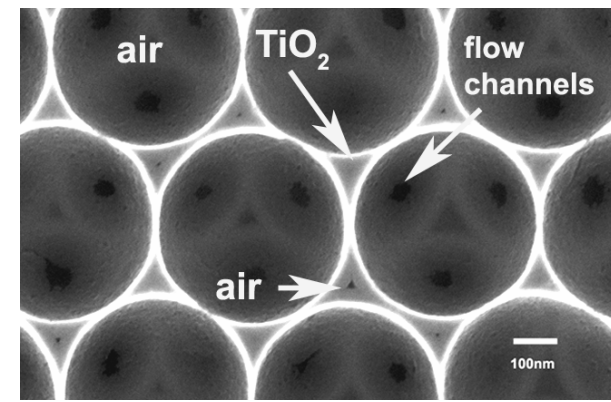
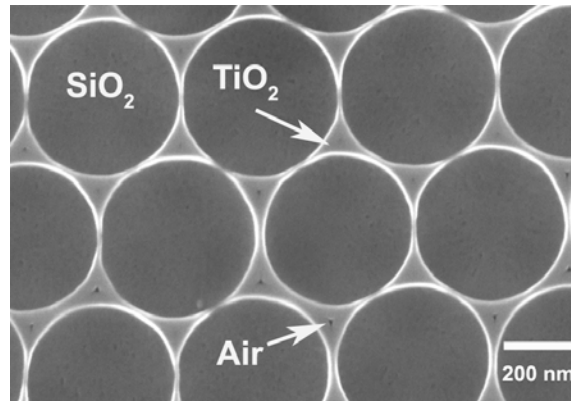
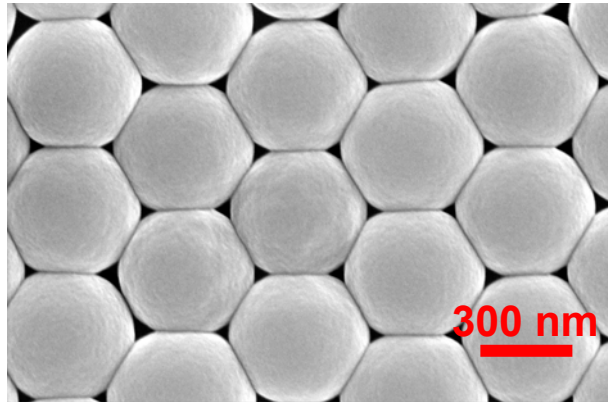


ALD of TiO_2 at 100°C



(111) \odot

Cross-sections



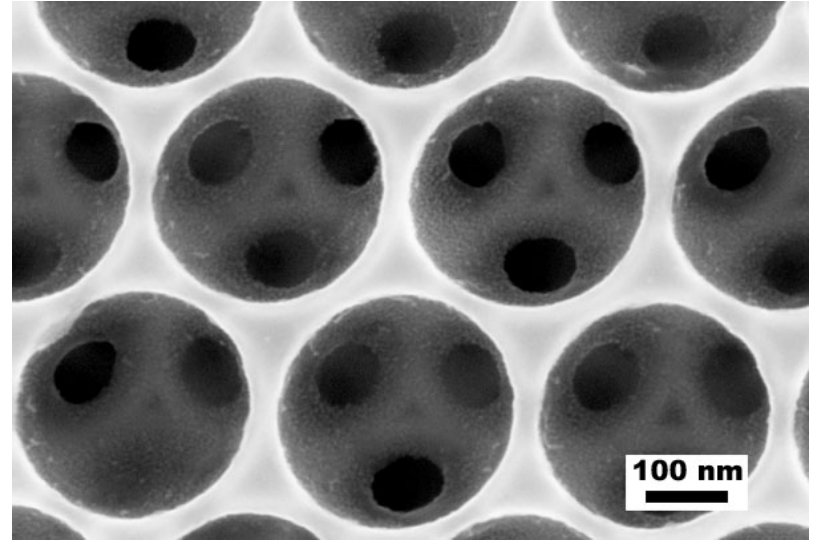
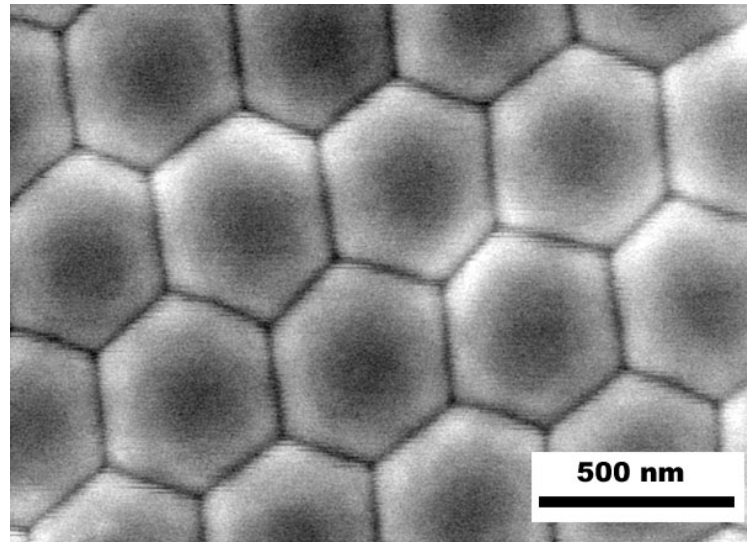
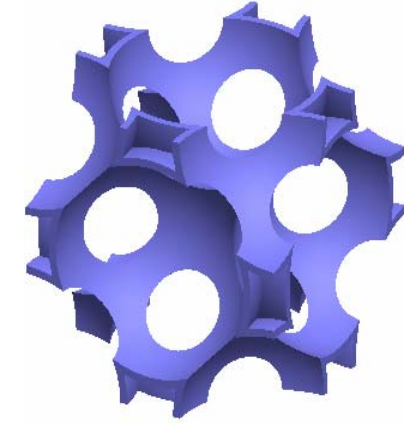
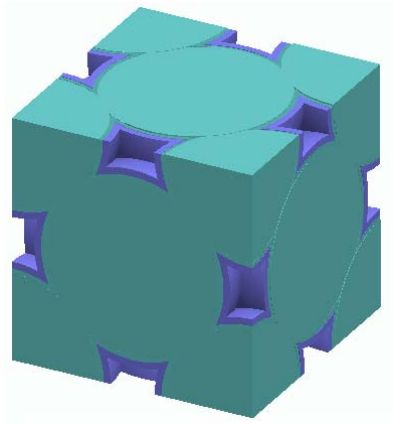
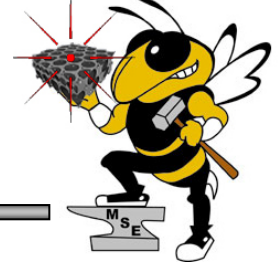
433 nm opal infiltrated
with 20 nm of TiO_2

433 nm opal infiltrated
with TiO_2

433 nm TiO_2 inverse opal

- TiO_2 infiltration at 100°C produces very smooth and conformal surface coatings with rms roughness $\sim 2\text{\AA}$.
- Heat treatment (400°C , 2 hrs.) of infiltrated opal converts it to anatase TiO_2 , increasing the refractive index from 2.35 to 2.65, with only a 2\AA increase in the rms surface roughness.

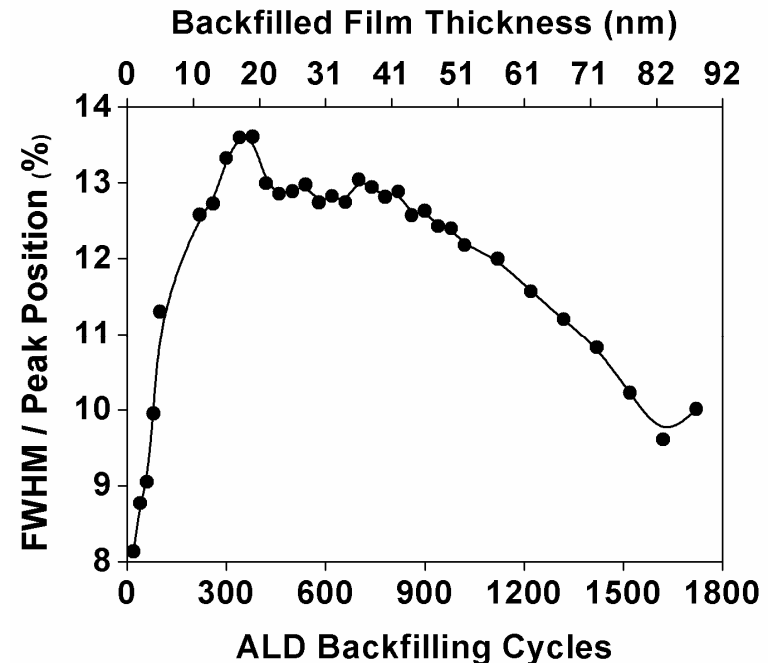
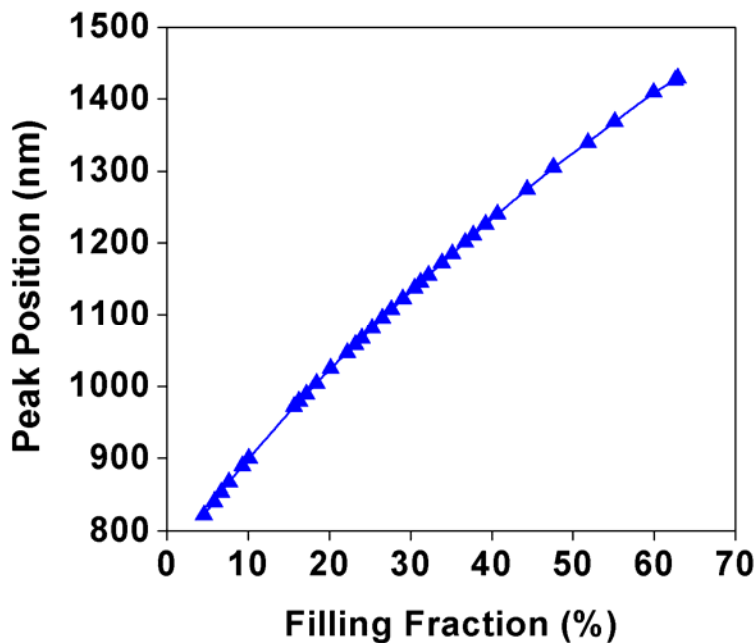
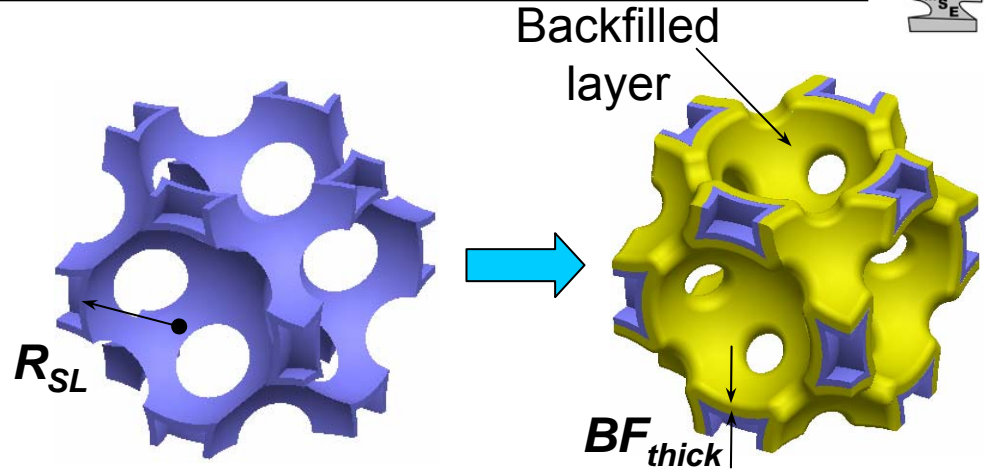
Pre-sintered Non-close-packed Inverse Shell Opals





Conformal Backfilling

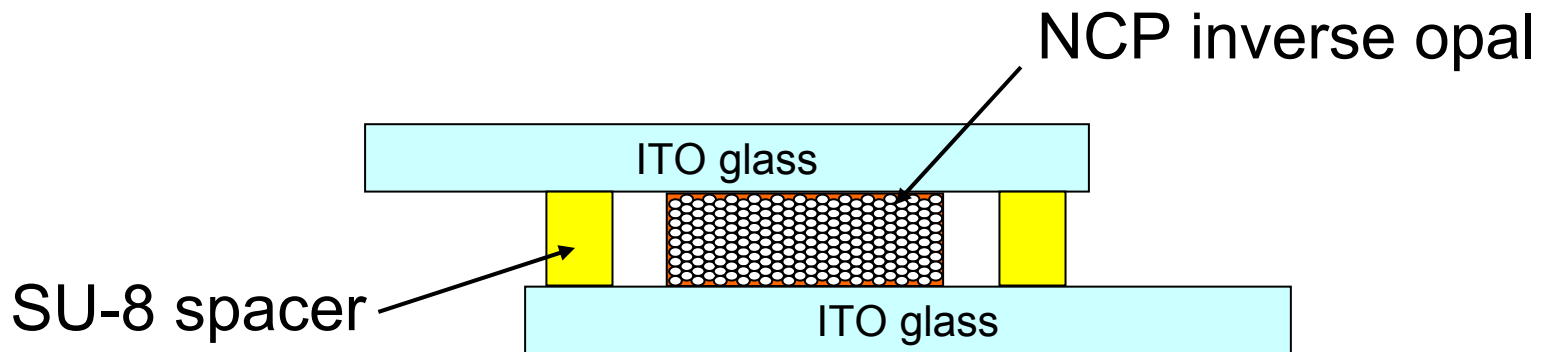
- ALD provides precise filling fraction control
- Over 600 nm tuning
- 167% Bragg peak width enhancement



Sample Cell Fabrication



- TiO_2 non-close-packed inverse shell opals were prepared using the sinter method.
- Several samples were coated with a hydrophobic surface treatment (fluorinated chlorosilane) to minimize surface pinning.
- Individual inverse opal grains were selected and placed between cleaned ITO coated glass substrates.
- Clean $10\ \mu\text{m}$ thick SU-8 spacers were used to separate the ITO surfaces.

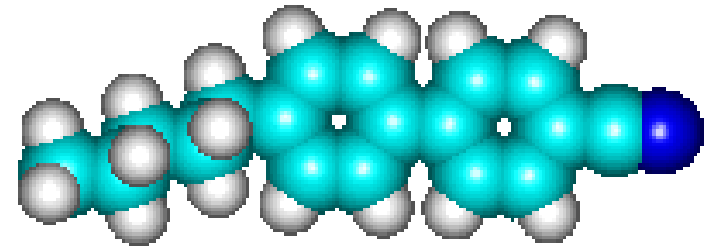
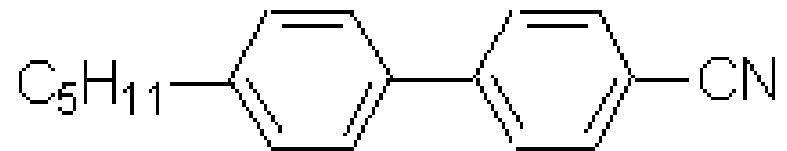




- Hydrophilic (untreated) samples
 - Infiltrated with pure 5CB at 50°C.
 - Drop at gap of the sample cell.
 - Immediate color change.

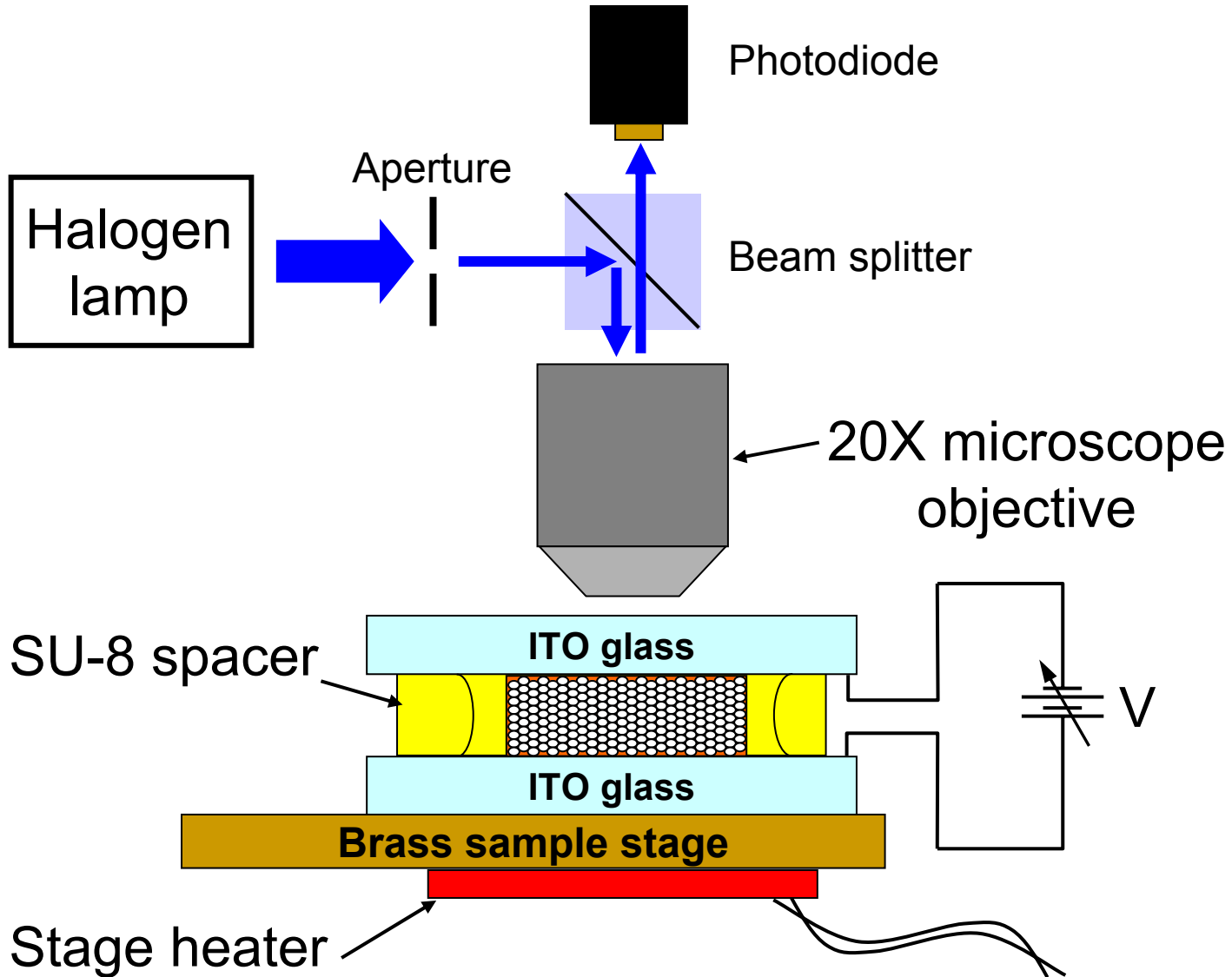
- Hydrophobic (treated) samples
 - Infiltrated with a mixture of 5% 5CB in ethanol at 20°C.
 - Drop at edge of partially open cell.
 - Gradual color change with repeated application
 - Post infiltration ensured ethanol removal.

5CB

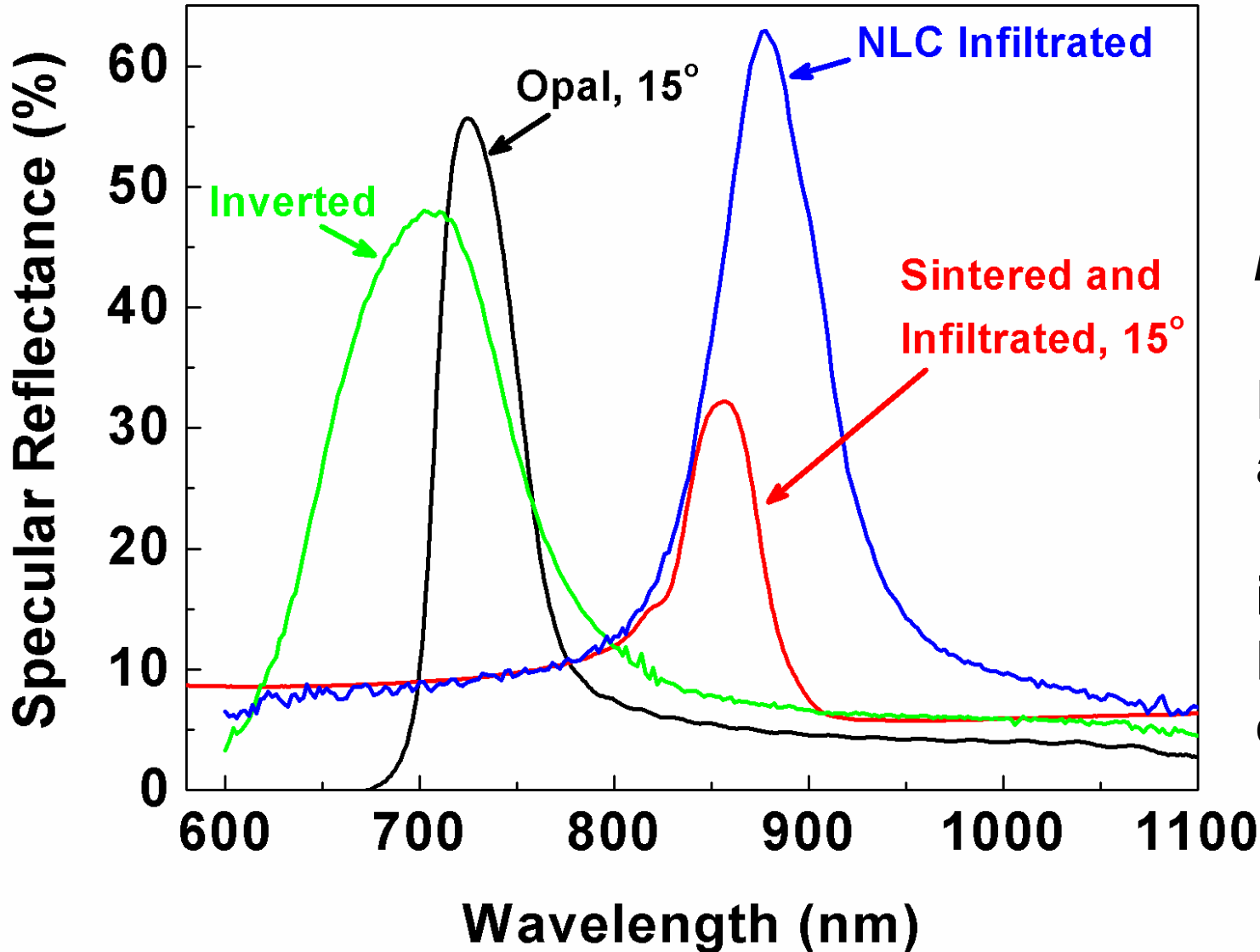


$$n = 1.522 \text{ to } 1.706$$

Schematic of microscope reflectance measurement



Reflectance Spectra



$$n_{ave}^{LC} = 1.586$$

$$n_{expt}^{LC} = 1.583$$

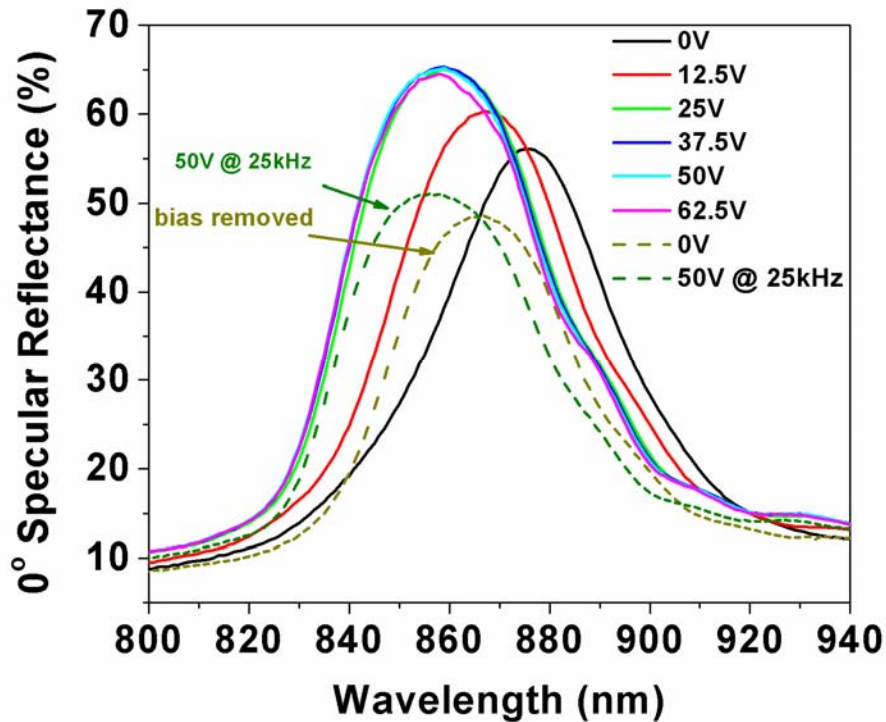
Excellent agreement
Indicates full infiltration and LC randomly oriented.

Electric Field Tuning: TiO₂ Non-close-packed inverse shell opals

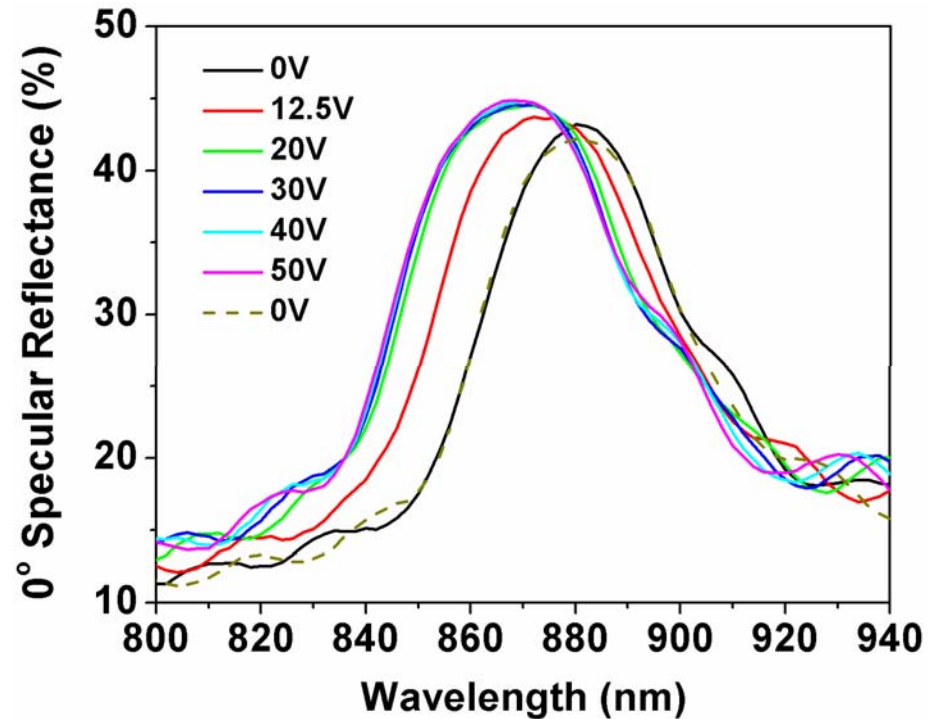


- Reflectance spectra for increasing applied electric field (bipolar square wave at 1 kHz) for NCPIO samples.

Hydrophobic treated



Hydrophilic

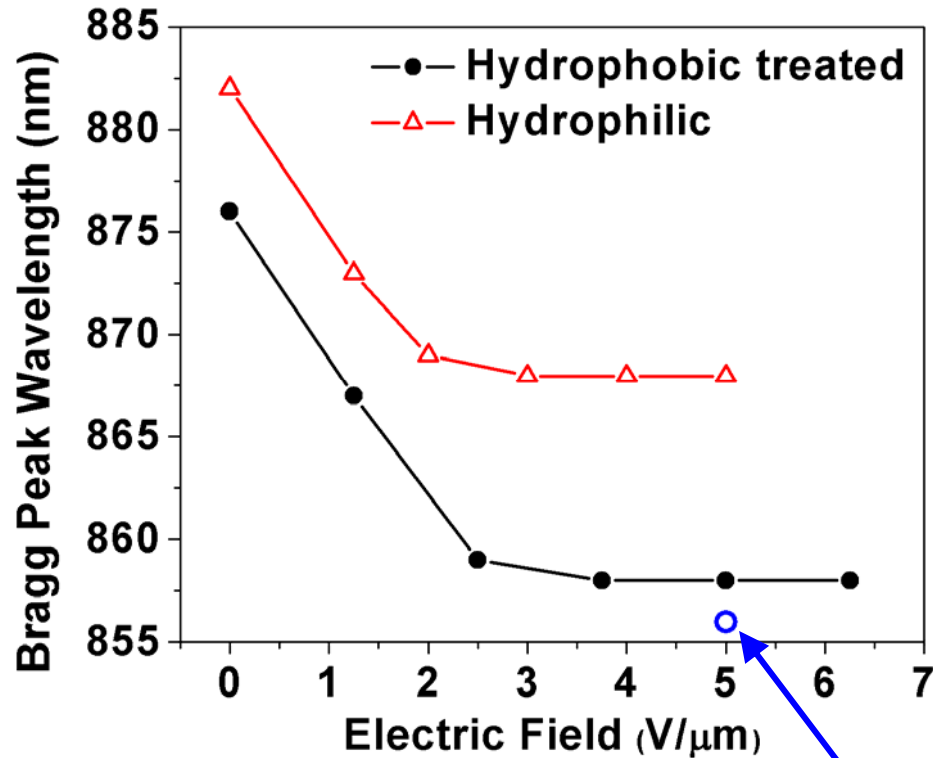


Electric Field Tuning



- Bragg peak position versus applied electric field at 1kHz

- Bragg peak width versus applied electric field at 1kHz



50V @ 25kHz → 856 nm



- Hydrophilic (untreated) sample:
 - 14 nm shift at 1 kHz
 - 14 nm shift at 25 kHz
 - Displays no hysteresis
- Hydrophobic sample:
 - Treated with fluorinated chlorosilane
 - 18 nm shift at 1 kHz
 - Gives $n_{LC} = 1.524$
 - 20 nm shift for 5 V/ μm at 25 kHz
 - Gives $n_{LC} = 1.518$
 - Displays hysteresis



- Experimental Results:
 - Peak Shift
 - Hydrophobic: 20 nm or Δn of 0.06
 - Hydrophilic: 14 nm
 - Peak Width Tunability
 - Hydrophobic: 0.91 %
 - Hydrophilic: 1.24 %
- Theoretical Predictions:
 - Peak Shift: 47 nm for $\Delta n = 0.1$ (28 nm for 0.06)
 - Peak Width Tunability: 1% for $\Delta n = 0.1$



-
- Theoretically calculated the expected performance for several opal based 3D PCs.
 - Predicted optimal structures for Bragg peak tunability or Bragg peak width – **Non-close-packed inverse opal.**
 - Observed a large 14 nm Bragg peak shift in high dielectric TiO₂ NCP structures.
 - Observed a larger 20 nm shift for NCP structures with a hydrophobic surface treatment.
 - Observed the maximum expected change of the refractive index for 5CB.
 - **Pathway to a tunable full photonic band gap:**
 - Higher index backbone
 - Larger Δn opto-electronic material

Acknowledgements



- Curtis Neff
- Dr. Brent Wagner

- Mike Ciftan/Rich Hammond,
U.S. Army Research Office
 - MURI “Intelligent Luminescence for
Communication, Display and Identification”
 - Contract DAAA19-01-1-0603